



In situ evaluation of gemcitabine–DNA interaction using a DNA-electrochemical biosensor

Rafael M. Buoro^{a,b}, Ilanna C. Lopes^a, Victor C. Diculescu^a, Silvia H.P. Serrano^b, Liseta Lemos^c, Ana Maria Oliveira-Brett^{a,*}

^a Departamento de Química, Faculdade de Ciências e Tecnologia, Universidade de Coimbra, 3004-535 Coimbra, Portugal

^b Departamento de Química Fundamental, Instituto de Química, Universidade de São Paulo, 05508-000 São Paulo, Brazil

^c Serviços Farmacêuticos, Centro Hospitalar e Universitário de Coimbra (CHUC), 3000-075 Coimbra, Portugal

ARTICLE INFO

Article history:

Received 14 February 2014

Received in revised form 9 May 2014

Accepted 30 May 2014

Available online 17 June 2014

Keywords:

Gemcitabine

DNA

Guanine

Electrochemical DNA-biosensor

Interaction mechanism

ABSTRACT

The electrochemical behaviour of the cytosine nucleoside analogue and anti-cancer drug gemcitabine (GEM) was investigated at glassy carbon electrode, using cyclic, differential pulse and square wave voltammetry, in different pH supporting electrolytes, and no electrochemical redox process was observed. The evaluation of the interaction between GEM and DNA in incubated solutions and using the DNA-electrochemical biosensor was studied. The DNA structural modifications and damage were electrochemically detected following the changes in the oxidation peaks of guanosine and adenosine residues and the occurrence of the free guanine residues electrochemical signal. The DNA–GEM interaction mechanism occurred in two sequential steps. The initial process was independent of the DNA sequence and led to the condensation/aggregation of the DNA strands, producing rigid structures, which favoured a second step, in which the guanine hydrogen atoms, participating in the C–G base pair, interacted with the GEM ribose moiety fluorine atoms.

© 2014 Elsevier B.V. All rights reserved.

1. Introduction

Nucleoside analogs of nucleobases are a pharmacological class of compounds with cytotoxic, immunosuppressive and antiviral properties [1], and the pyrimidine nucleoside analogs are relevant derivatives effective in cancer treatment.

Gemcitabine (GEM), 2,2-difluorodeoxycytidine, Scheme 1A, is a nucleoside analogue of cytidine, Scheme 1B, and plays a major role in the treatment of bladder and breast [1–4] cancer, and when combined with doxorubicin in hepatic [5], non-small cell lung and pancreatic cancer [6–8].

Due to its lipophilic characteristic, GEM is easily transported inside the cell by nucleoside membrane transporters where it is phosphorylated and then competes with cytidine derivatives in the DNA synthesis. A high concentration of GEM triphosphate inhibits cytidine triphosphate (CTP) synthetase, and cytidine monophosphate (CMP) deaminase, which maintain CTP in low concentrations [1] and assures greater availability of GEM triphosphate. GEM mainly exerts its biological activity by two mechanisms. The first pathway corresponds to the incorporation of GEM into DNA triggering the mechanism of DNA repairing, but the

enzyme responsible for the base excision is not capable of removing GEM and replication stops [1]. In the second pathway blocking of DNA synthesis, through the inhibition of ribonucleotide reductase occurs, impeding the synthesis of the new strand.

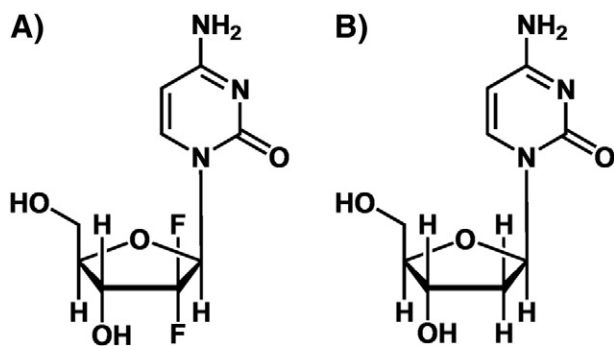
GEM compared to the other drugs used on cancer treatment, in mono- and combined chemotherapies, is well tolerated among patients, with acceptable side effects and toxicity [5–8]. Due to the positive aspects of nucleoside analogs in several types of cancer treatment, their analytical determination is an important issue. Electroanalytical methods have been previously used for the characterization of purine nucleosides analogues, such as claribidine [9], clorafabine [10] and fludarabine [11], and the influence of the structural differences in the ribose moiety on their electrochemical behaviour investigated. HPLC–MS and UV–vis spectrophotometry were also applied for the determination and quantization of GEM [12–14].

The interaction of some purine nucleosides with DNA has been previously studied in incubated solutions and with a DNA-electrochemical biosensor [9–11]. Interaction of the damaging agent with DNA caused changes into the properties of the DNA recognition layer and this effect was quantified electrochemically [15–18]. It has been shown that the nucleoside analog caused dsDNA structural modifications in a time-dependent manner, but no DNA oxidative damage [9,10].

Although the DNA damage mechanism by nucleoside analogues apparently involved secondary biochemical reactions there are studies

* Corresponding author. Tel./fax: +351 239 835295.

E-mail address: brett@ci.uc.pt (A.M. Oliveira-Brett).



Scheme 1. Chemical structure: A) gemcitabine (GEM) and B) cytidine.

indicating that may lead to processes giving rise to or inducing disruption or breakages of the genetic material [9–11]. Accumulation of DNA damage increases carcinogenic risk and may result in a malignant transformation or cell death. Therefore, the study of a direct interaction between dsDNA and GEM should be undertaken.

This paper investigates the GEM electrochemical behaviour at a glassy carbon electrode by cyclic, differential pulse and square wave voltammetry, and the DNA–GEM interaction as function of incubation time, in incubated solutions, and with the dsDNA-electrochemical biosensor, using differential pulse voltammetry.

2. Experimental

2.1. Materials and reagents

Gemcitabine–Gemzar (GEM) was obtained from Lilly LLC laboratories. Sodium salt double stranded DNA (dsDNA) from calf thymus, guanosine, polyguanylic salt (poly[G]) and polyadenylic salt (poly[A]) were obtained from Sigma–Aldrich and used without further purification.

Stock solutions of 100 μM GEM, 1.0 mM guanosine, 187 $\mu\text{g mL}^{-1}$ dsDNA, 504 $\mu\text{g mL}^{-1}$ poly[G] and 521 $\mu\text{g mL}^{-1}$ poly[A] were prepared in deionized water and kept at 4 $^{\circ}\text{C}$, and solutions of different concentrations were prepared by dilution in 0.1 M acetate buffer pH = 4.5.

All supporting electrolyte solutions: HCl + KCl pH's 1.2 and 2.0; HAc + NaAc pH's 3.1, 4.5 and 5.4; NaH_2PO_4 + Na_2HPO_4 pH's 6.2, 7.1 and 8.2; NH_3 + NH_4Cl pH's 9.1, 10.2 and 11.0, were prepared using analytical grade reagents and purified water from Millipore Milli-Q system (conductivity $\leq 0.1 \mu\text{S cm}^{-1}$).

The pH measurements were carried out using a Crison microPH 2001 pH-meter with Ingold combined glass electrode. All experiments were done at room temperature (25 ± 1 $^{\circ}\text{C}$) and microvolumes were measured using EP-10 and EP-100 Plus Motorized Microliter Pippettes (Raining Instrument Co. Inc., Woburn, USA).

2.2. Voltammetric parameters and electrochemical cells

Voltammetric experiments were carried out using an Autolab PGStat 10 running GPES 4.9 software, Eco-Chemie, Utrecht, The Netherlands. Measurements were carried out using a glassy carbon working electrode (GCE) ($d = 1$ mm), a Pt wire counter electrode, and an Ag/AgCl (3 M KCl) reference electrode, in a one-compartment 3 mL electrochemical cell (eDAQ Products, Poland). The experimental conditions for differential pulse (DP) voltammetry were: pulse amplitude 50 mV, pulse width 70 ms, potential increment of 2 mV and scan rate 5 mV s^{-1} . For square wave (SW) voltammetry: a pulse amplitude of 50 mV, a potential increment of 2 mV, and a frequency of 50 Hz for an effective scan rate of 100 mV s^{-1} .

Prior to each measurement and preparation of each biosensor, the GCE was polished using diamond spray (UK Kemet, particle size 1 μm). After polishing, the electrode surface was rinsed thoroughly with Milli-Q water. Following the mechanical treatment, the GCE was

placed in support electrolyte and voltammograms were recorded until a steady state baseline voltammogram was obtained. This procedure ensured very reproducible experimental results.

2.3. Acquisition and presentation of data

All the voltammograms presented were baseline corrected using the moving average with a step window of 2 mV included in GPES version 4.9 software. This mathematical treatment improves the visualization and identification of peaks over the baseline without introducing any artefact, although the peak height is in some cases reduced ($<10\%$) relative to that of the untreated curve. Nevertheless, this mathematical treatment of the original voltammograms was used in the presentation of all experimental voltammograms for a better and clearer identification of the peaks. The values for peak current presented in all graphs were determined from the original untreated voltammograms after subtraction of the baseline.

2.4. Incubation procedures

2.4.1. Procedure 1—incubated solutions

The experimental conditions were 50 $\mu\text{g mL}^{-1}$ dsDNA, poly[G] or poly[A] that were separately incubated with 10 μM GEM during different time periods. In order to explain the interaction mechanism between GEM and DNA, solutions of 25 μM GEM were separately incubated with 25 μM guanosine, cytidine or adenosine in 0.1 M acetate buffer pH = 4.5 during different time periods.

Two types of control experiments were performed. In one control experiment different solutions of 10 μM GEM, 50 $\mu\text{g mL}^{-1}$ dsDNA, poly[G], poly[A] and 25 μM guanosine, cytidine or adenosine were separately prepared and stored in similar conditions and during the same time periods as the incubated solutions. In the other control experiment, different solutions of 50 $\mu\text{g mL}^{-1}$ dsDNA or 25 μM guanosine were incubated during 4 h with 25 μM cytidine.

The interaction between GEM and poly[G], poly[A], guanosine or adenosine was studied in order to identify possible specific interactions between the nucleoside derivative and a specific DNA base.

2.4.2. Procedure 2—dsDNA-electrochemical biosensor

The dsDNA-electrochemical biosensors were prepared by covering successively the GCE surface with three drops each of 5 μL from a 50 $\mu\text{g mL}^{-1}$ dsDNA solution diluted in 0.1 M acetate buffer pH = 4.5. After placing each drop on the electrode surface the biosensor was dried under a constant flux of N_2 . A similar procedure was used in order to obtain the poly[G] and poly[A]-electrochemical biosensors.

This procedure ensures full coverage of the electrode surface necessary to avoid the formation of undesired thin and incomplete network film of co-adsorbed dsDNA–GEM, dsDNA or GEM nonspecific binding to the electrode surface.

The biosensor was immersed and allowed to incubate in a solution of 10 μM GEM in 0.1 M acetate buffer pH = 4.5, during different time periods. Afterwards, the electrochemical biosensors were removed from the solution, washed with deionized water in order to remove the unbounded GEM molecules and placed in the electrochemical cell containing only the supporting electrolyte 0.1 M acetate buffer pH = 4.5, where DP voltammetry was performed.

For control experiments, the dsDNA-electrochemical biosensor was incubated during 4 h either in buffer or in a solution of 25 μM cytidine.

2.5. Spectrophotometric parameters

The UV–vis measurements were performed using a spectrophotometer SPECORD S100, running with Aspect Plus Version 1.5 (Analytik Jena GmbH, Jena, Germany). The experimental conditions for absorption spectra were: integration time 25 ms and accumulation 1000 points. All UV–vis spectra were measured from 230 nm to 330 nm, in a quartz

glass cuvette with an optic path of 1 cm. UV–vis spectra were recorded for different incubation times of 10 μM of GEM and 50 $\mu\text{g mL}^{-1}$ dsDNA in 0.1 M acetate buffer pH 4.5. Control solutions of 50 $\mu\text{g mL}^{-1}$ dsDNA or 10 μM GEM were also prepared and UV–vis spectra were recorded for the same time periods.

3. Results and discussion

3.1. Electrochemical behaviour of gemcitabine, dsDNA, poly[G] and poly[A]

The electrochemical behaviour of GEM was investigated by cyclic, DP, and SW voltammetry in solutions of 50 μM GEM in electrolytes with pH values between 1.0 and 11.0, and no electrochemical process related to GEM oxidation or reduction at the glassy carbon electrode in the potential range between -0.70 and $+1.40$ V was observed (Fig. 1).

The DP voltammogram of dsDNA showed two well defined peaks corresponding to the oxidation of desoxyguanosine (dGuo), at $E_{\text{pa}} =$

$+0.98$ V, and desoxyadenosine (dAdo), at $E_{\text{pa}} = +1.25$ V. The DP voltammogram of poly[G] presented only the dGuo peak and of poly[A] showed only the dAdo peak, at the same potentials as observed for the dsDNA solution although with greater currents (Fig. 1).

3.2. Evaluation of GEM–dsDNA interaction in incubated solutions

3.2.1. Electrochemical measurements

The electrochemical study of the GEM–dsDNA interaction was carried out in incubated solutions containing 10 μM GEM and 50 $\mu\text{g mL}^{-1}$ dsDNA in 0.1 M acetate buffer solution, pH = 4.5.

The nucleoside analogue concentration was established according to the minimum concentration of GEM in the infusion solution in chemotherapy procedure which is 0.1 mg/mL (380 μM). Considering the uptake of cells for the nucleoside analogues, the final concentration in cell will not surpass 10 μM . Even though, studies of the interaction between 100 μM GEM and dsDNA were performed and the same behaviour of condensation and/or aggregation observed for 10 μM of GEM, but for shorter periods of time.

The DP voltammogram recorded immediately after the addition of GEM to the dsDNA solution showed the decrease of dGuo and dAdo oxidation peak currents (Fig. 2), when compared with the control dsDNA solution. Increasing the incubation time, both dGuo and dAdo oxidation peaks decreased.

A similar behaviour was observed for incubated solutions of GEM with poly[G] and poly[A]. In poly[G] a shift of ~ 40 mV of the dGuo oxidation peak and a small new oxidation peak, at $E_{\text{pa}} = +0.76$ V (Fig. 3A), indicating a preferential interaction between GEM and guanine (Fig. 3A and B), was observed.

The DP voltammogram recorded in 25 μM guanosine incubated during 4 h with 25 μM GEM showed the shift to a more positive potential, the decrease of dGuo oxidation peak current, and the new peak corresponding to free guanine residue oxidation, at $E_{\text{pa}} = +0.76$ V (Fig. 4).

The occurrence of the free guanine peak is explained considering the GEM-induced cleavage of the bond between guanine and the sugar moiety in the guanosine residues, leading to the release of guanine which is oxidized at a lower potential [19,20]. The same procedure of incubation was performed with adenosine and no modifications were observed.

A control experiment of 25 μM guanosine with 25 μM cytidine was performed and the results indicate no release of guanine after 4 h of incubation.

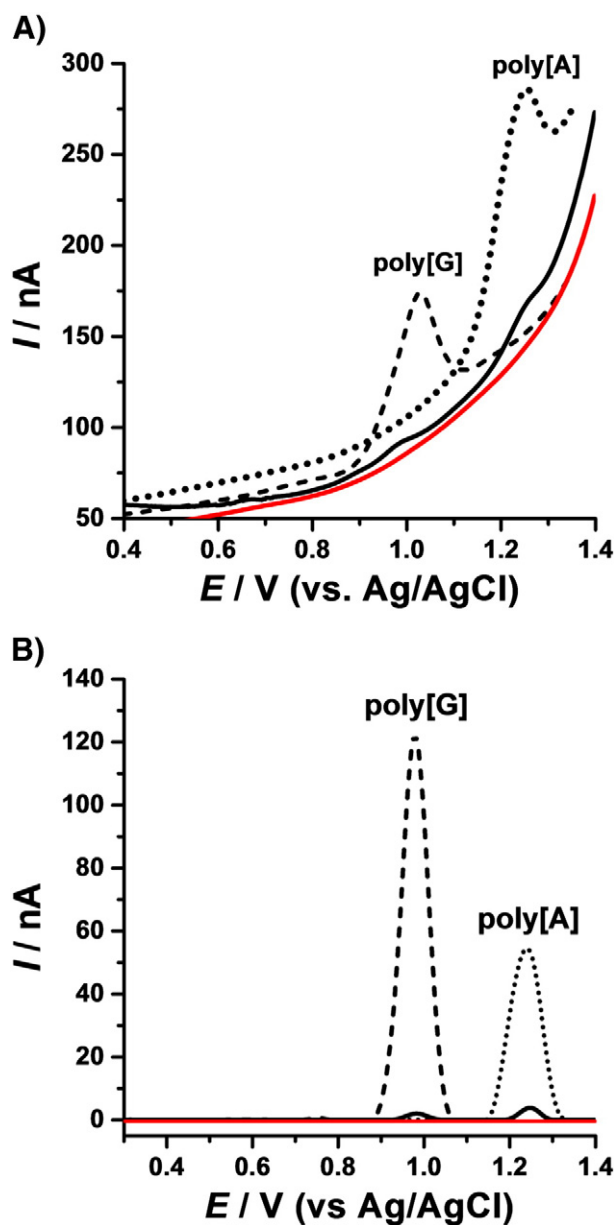


Fig. 1. DP voltammograms in 0.1 M acetate buffer solution pH 4.5, of 50 $\mu\text{g mL}^{-1}$: (—) dsDNA, (---) poly[G] and (···) poly[A], and (—) 50 μM GEM: (A) without baseline-correction and (B) with baseline-correction. Scan rate 5 mV/s.

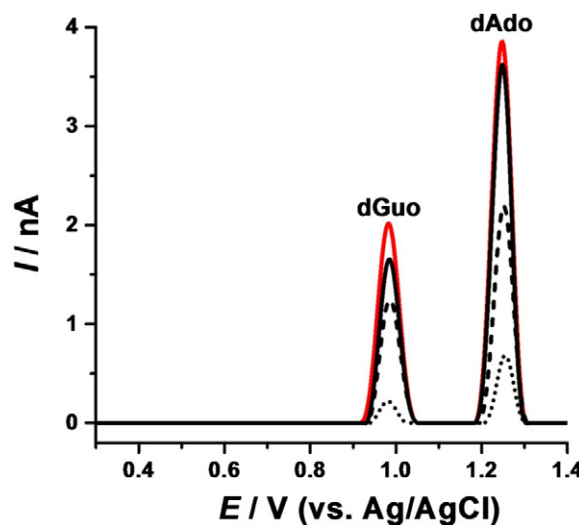


Fig. 2. DP voltammograms baseline-corrected in 0.1 M acetate buffer pH = 4.5, in (—) 50 $\mu\text{g mL}^{-1}$ dsDNA and after incubation of 50 $\mu\text{g mL}^{-1}$ dsDNA with 10 μM GEM during (—) 0 h, (---) 2 h and (···) 4 h. Scan rate 5 mV/s.

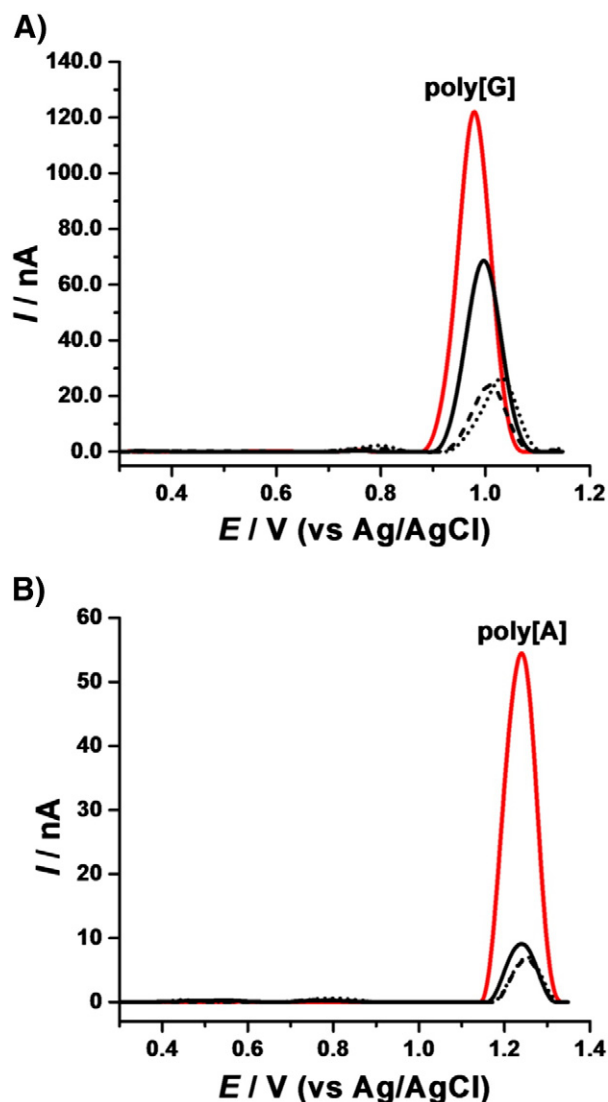


Fig. 3. DP voltammograms baseline-corrected in $50 \mu\text{g mL}^{-1}$: A) poly[G] and B) poly[A], in 0.1 M acetate buffer pH = 4.5, (—) before and after incubation with $10 \mu\text{M}$ GEM during (—) 0 h, (---) 2 h and (···) 4 h. Scan rate 5 mV/s.

3.2.2. UV-vis spectrophotometry

The UV-vis study of the GEM-dsDNA interaction was carried out in incubate solutions of $10 \mu\text{M}$ GEM and $50 \mu\text{g mL}^{-1}$ dsDNA, in 0.1 M acetate buffer pH = 4.5. UV-vis spectra were recorded after different incubation periods (Fig. 5). Control solutions of $50 \mu\text{g mL}^{-1}$ dsDNA and $10 \mu\text{M}$ of GEM were also prepared and UV-vis spectra were recorded for the same incubation times.

The UV-vis spectra obtained in a freshly prepared solution of GEM showed an absorption band at $\lambda = 270.2 \text{ nm}$, close to the maximum absorption of dsDNA, at $\lambda = 259.9 \text{ nm}$ (Fig. 5) that decreased after 24 h incubation, in agreement with condensation/aggregation of dsDNA upon interaction with GEM as observed in the electrochemical experiments.

3.3. dsDNA-electrochemical biosensor in situ sensing of GEM-dsDNA interaction

Ensuring full coverage of the electrode surface was necessary to avoid the formation of undesired thin and incomplete network film of co-adsorbed dsDNA-GEM, dsDNA or GEM nonspecific binding to the electrode surface [19]. The dsDNA-electrochemical biosensor enabled to detect *in situ* and in real time [19,20] the changes occurring to the

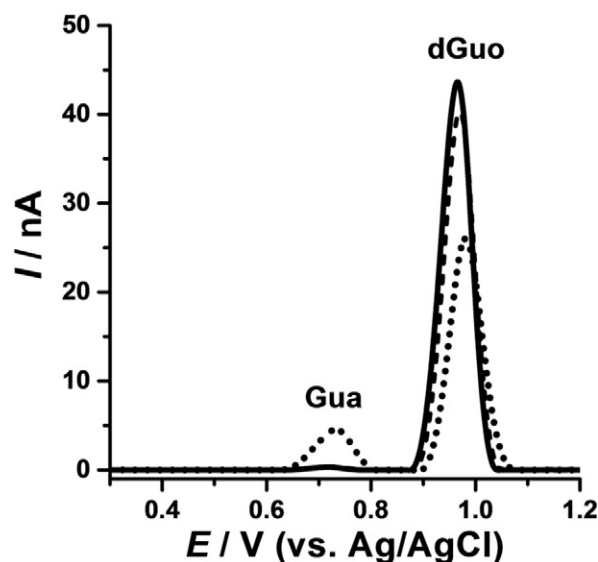


Fig. 4. DP voltammograms baseline-corrected in 0.1 M acetate buffer pH = 4.5, in $25 \mu\text{M}$ guanosine (—) before and after 4 h incubation with $25 \mu\text{M}$ (···) GEM or (---) cytidine. Scan rate 5 mV/s.

dsDNA immobilized on the electrode surface during the interaction with GEM.

The DP voltammogram for the control dsDNA-electrochemical biosensor showed both dGuo and dAdo oxidation peaks (Fig. 6). After incubation for a period of time in $10 \mu\text{M}$ GEM the dsDNA-electrochemical biosensor was carefully washed with deionized water, to remove unbound GEM molecules, and transferred to only the 0.1 M acetate buffer supporting electrolyte solution. The experiment was repeated, always with a new dsDNA-electrochemical biosensor, for different incubation times (Fig. 6).

The peaks corresponding to the oxidation of dGuo, at $E_{\text{pa}} = +0.98 \text{ V}$, and dAdo, at $E_{\text{pa}} = +1.25 \text{ V}$, decreased up to 4 h incubation. At the same time, the shift of the dGuo oxidation peak indicated a preferential interaction between GEM and dGuo residues in the dsDNA. The release of free guanine, oxidation peak at $E_{\text{pa}} = +0.76 \text{ V}$, was also observed.

In the control experiments after 24 h incubation in buffer solution in the same conditions no significant variation on the dGuo and dAdo oxidation peaks was observed. A control incubation of the dsDNA-electrochemical biosensors in $25 \mu\text{M}$ of cytidine during 4 h

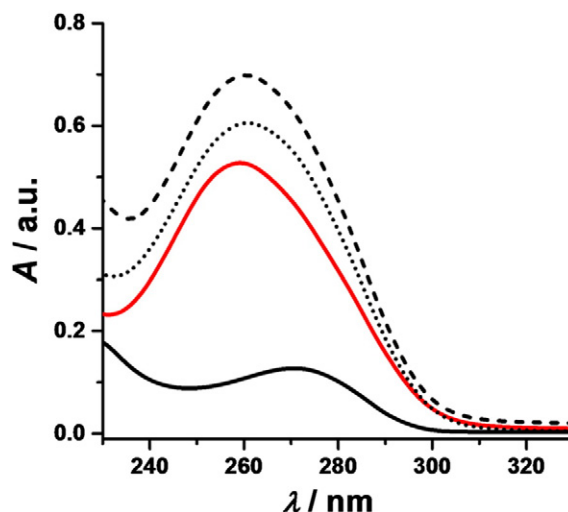


Fig. 5. UV-vis absorption spectra: (—) $50 \mu\text{g mL}^{-1}$ dsDNA, (—) $10 \mu\text{M}$ GEM, and after incubation of $50 \mu\text{g mL}^{-1}$ dsDNA and $10 \mu\text{M}$ GEM during (---) 0 h and (···) 24 h.

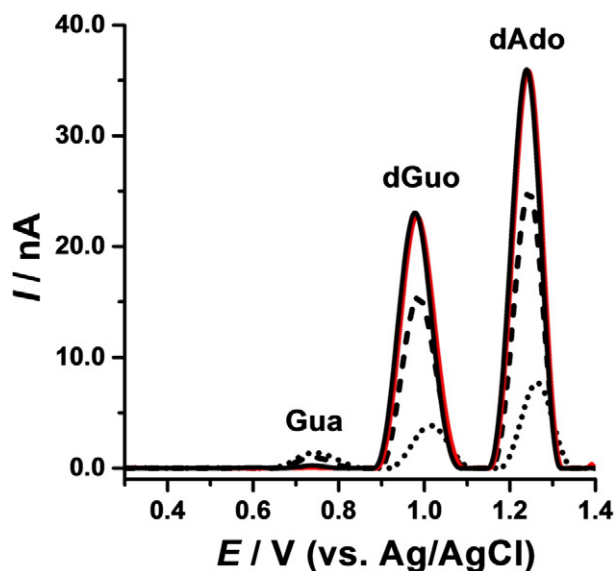


Fig. 6. DP voltammograms baseline-corrected in 0.1 M acetate buffer pH = 4.5: dsDNA-electrochemical biosensor (—) control and after incubation with 10 μ M GEM during (---) 2 h and (···) 4 h, and with after incubation (—) 25 μ M of cytidine during 4 h. Scan rate 5 mV/s.

showed no change of the peaks corresponding to the oxidation of dGuo and dAdo.

Previous studies [15,21] on the electrochemical behaviour of double stranded DNA (dsDNA) and single stranded DNA (ssDNA) illustrated the greater difficulty for the transfer of electrons from the inside of the double-stranded rigid form of DNA to the electrode surface, than from the flexible single stranded form of DNA where the bases are in close proximity to the electrode surface.

The decrease of DNA oxidation peaks observed after the interaction with GEM is due to the formation of a more compact DNA structure. This behaviour is consistent with the aggregation/condensation of the dsDNA, promoted by the interaction with GEM, and in agreement with spectrophotometric measurements (Fig. 5). The formation of rigid GEM–DNA structures hinders the nucleoside residues to interact and oxidize at the GCE surface.

The dsDNA-electrochemical biosensor incubated in solutions of 100 μ M GEM presented a similar behaviour, and the condensation of dsDNA was achieved for shorter incubation times.

No DNA oxidative damage, concerning the occurrence of the oxidation peaks of 8-oxoguanine (8-oxoGua) or 2,8-dihydroxyadenine (2,8-oxoAde), was observed. This means that GEM did not induce oxidative damage to dsDNA.

In order to obtain information on the preferential interaction of GEM with dsDNA, the GCE surface was modified with polyhomonucleotides, the poly[G] or poly[A]-electrochemical biosensors.

The poly[G]-electrochemical biosensors showed only one peak corresponding to the oxidation of dGuo, at $E_{pa} = +0.98$ V (Fig. 7A), which decreased after incubation in 10 μ M GEM, and the guanine oxidation peak, at $E_{pa} = +0.76$ V, appeared (Fig. 7A), indicating the release of free guanine bases.

Similar results were observed using poly[A]-electrochemical biosensors incubated with GEM; the dAdo oxidation peak, at $E_{pa} = +1.24$ V, decreased but no additional peak at a lower positive potential was observed.

The interaction mechanism GEM–DNA occurs in two consecutive steps. The initial step is independent of the DNA sequence, and leads to the condensation/aggregation of DNA strands [21]. In the second step, a preferential interaction between the guanine hydrogen atoms in the C–G base pair and the fluorine atoms in the GEM ribose moiety,

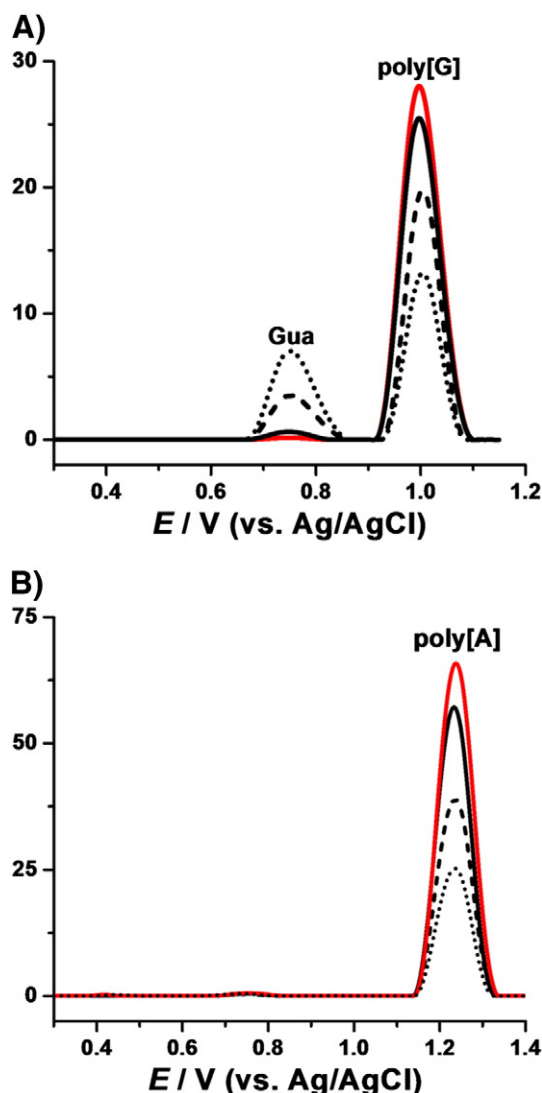


Fig. 7. DP voltammograms baseline-corrected in 0.1 M acetate buffer pH = 4.5: A) poly[G] and B) poly[A]-electrochemical biosensors and 10 μ M GEM after incubation during (—) 0, (---) 15 min, (···) 2 h and (— · —) 4 h. Scan rate 5 mV/s.

caused the release and/or exposure of guanine residues to the electrode surface to occur.

4. Conclusions

The electrochemical behaviour of the anti-cancer drug gemcitabine (GEM) was investigated and no electrochemical process was observed. The interaction DNA–GEM was investigated in incubated solutions and with a DNA-electrochemical biosensor, and caused modifications in the DNA morphological structure, which were also observed when using polyhomonucleotides of guanosine and adenosine, poly[G] and poly[A]-electrochemical biosensors. The DNA–GEM interaction mechanism occurred in two consecutive steps. The initial process was independent of the DNA sequence and led to the condensation/aggregation of dsDNA. The formation of a GEM–DNA rigid structure promoted a second step favouring the interaction between the guanine hydrogen atom participants in the C–G base pair and the fluorine atoms in the gemcitabine ribose moiety and provoking the release and/or exposure of guanine residues to the electrode surface. In addition, GEM also did not induce oxidative damage to DNA.

Acknowledgements

Financial support from: Fundação para a Ciência e Tecnologia (FCT)—Portugal, projects PTDC/QEQ-MED/0586/2012, PTDC/DTP-FTO/0191/2012, PEst-C/EME/UI0285/2013 and CENTRO-07-0224-FEDER-002001 (MT4MOBI) (co-financed by the European Community Fund FEDER), FEDER funds through the program COMPETE—Programa Operacional Factores de Competitividade, CAPES—Brazil, PhD Grant/18796/12-5 (R.M. Buoro) and CNPq—Brazil, Post-Doctoral Grant/201487/2011-0 (I.C. Lopes), is gratefully acknowledged.

References

- [1] C.M. Galmarini, J.R. Mackey, C. Dumontet, Nucleoside analogues and nucleobases in cancer treatment, *Lancet Oncol.* 3 (2002) 415–424.
- [2] J. Carmichael, J. Walling, Advanced breast cancer: investigational role of gemcitabine, *Eur. J. Cancer* 33 (1997) S27–S30.
- [3] M.D. Shelley, A. Cleves, T.J. Wilt, M.D. Mason, Gemcitabine chemotherapy for the treatment of metastatic bladder carcinoma, *BJU Int.* 108 (2011) 168–179.
- [4] T. Walter, A.M. Horgan, M. McNamara, L. McKeever, T. Min, D. Hedley, S. Serra, M.K. Krzyzanowska, E. Chen, H. Mackay, R. Feld, M. Moore, J.J. Knox, Feasibility and benefits of second-line chemotherapy in advanced biliary tract cancer: a large retrospective study, *Eur. J. Cancer* 49 (2013) 329–335.
- [5] G. Lombardi, F. Zustovich, F. Farinati, U. Cillo, A. Vitale, G. Zanusi, M. Donach, M. Farina, S. Zovato, D. Pastorelli, Pegylated liposomal doxorubicin and gemcitabine in patients with advanced hepatocellular carcinoma: results of a phase 2 study, *Cancer* 117 (1) (2011) 125–133.
- [6] A. Maraveyas, J. Waters, R. Roy, D. Fyfe, D. Propper, F. Lofts, J. Sgouros, E. Gardiner, K. Wedgwood, C. Ettelaie, G. Bozas, Gemcitabine versus gemcitabine plus dalteparin thromboprophylaxis in pancreatic cancer, *Eur. J. Cancer* 48 (2012) 1283–1292.
- [7] H.Q. Xiong, A. Rosenberg, A. LoBuglio, W. Schmidt, R.A. Wolff, J. Deutsch, M. Needle, J.L. Abbruzzese, Cetuximab, a monoclonal antibody targeting the epidermal growth factor receptor, in combination with gemcitabine for advanced pancreatic cancer: a multicenter phase II trial, *J. Clin. Oncol.* 22 (13) (2004) 2610–2616.
- [8] J.E. Frampton, A.J. Wagstaff, Gemcitabine: a review of its use in the management of pancreatic cancer, *Am. J. Cancer* 4 (6) (2006) 395–416.
- [9] H.E. Satana, A.D.R. Pontinha, V.C. Diclescu, A.M. Oliveira Brett, Nucleoside analogue electrochemical behaviour and in situ valuation of DNA–clorafabine interaction, *Bioelectrochemistry* 87 (2012) 3–8.
- [10] A.D.R. Pontinha, H.E. Satana, V.C. Diclescu, A.M. Oliveira Brett, Anodic oxidation of cladribine and in situ evaluation of DNA–cladribine interaction, *Electroanalysis* 23 (11) (2011) 2651–2657.
- [11] H.E. Satana, A.M. Oliveira Brett, *In situ* evaluation of fludarabine–DNA interaction using a DNA-electrochemical biosensor, *Int. J. Electrochem.* 2011 (2011) 1–8.
- [12] R. Losa, M.I. Sierra, M.O. Gi6n, E. Esteban, J.M. Buesa, Simultaneous determination of gemcitabine di- and triphosphate in human blood mononuclear and cancer cells by RP-HPLC and UV-detection, *J. Chromatogr. B* 840 (2006) 44–49.
- [13] R. Honeywell, A.C. Laan, C.J. van Groenigen, E. Strocchi, R. Ruiter, G. Giaccone, G.J. Peters, The determination of gemcitabine and 2'-deoxycytidine in human plasma and tissue by APCI tandem mass spectrometry, *J. Chromatogr. B* 847 (2007) 142–152.
- [14] M.N. Kirstein, I. Hassan, D.E. Guire, D.R. Weller, J.W. Dagit, J.E. Fischer, R.P. Rimmel, High Performance liquid chromatographic method for the determination of gemcitabine and 2',2'-difluorodeoxyuridine in plasma and tissue culture media, *J. Chromatogr. B* 835 (2006) 136–142.
- [15] V.C. Diclescu, M. Vivian, A.M. Oliveira Brett, Voltammetric behaviour of antileukemia drug Glivec. Part III: In situ DNA oxidative damage by Glivec electrochemical metabolite, *Electroanalysis* 18 (19–20) (2006) 1963–1970.
- [16] A.M. Oliveira Brett, A.M. Chiorcea-Paquim, V.C. Diclescu, J.A.P. Piedade, Electrochemistry of nanoscale DNA surface films on carbon, *Med. Eng. Phys.* 10 (2006) 963–970.
- [17] V.C. Diclescu, J.A.P. Piedade, A.M. Oliveira Brett, Electrochemical behaviour of 2,8-dihydroxyadenine at a glassy carbon electrode, *Bioelectrochemistry* 70 (2007) 141–146.
- [18] A.M. Oliveira Brett, M. Vivan, I.R. Fernandes, J.A.P. Piedade, Electrochemical detection of in situ adriamycin oxidative damage to DNA, *Talanta* 56 (2002) 959–970.
- [19] V.C. Diclescu, A.M. Oliveira Brett, Chapter 10—DNA-electrochemical biosensors and oxidative damage to DNA: application to cancer. Section 2: blood, molecules and cells, in: V.R. Preedy (Ed.), *Biosensors and Cancer*, Science Publisher, CRC Press, New Hampshire, USA, 2012.
- [20] A.M. Oliveira Brett, S.H.P. Serrano, T.A. Macedo, D. Raimundo, M.H. Marques, M.A. La-Scalea, Electrochemical determination of carboplatin in serum using a DNA-modified glassy carbon electrode, *Electroanalysis* 8 (11) (1996) 992–995.
- [21] S.C.B. Oliveira, A.M. Chiorcea-Paquim, S.M. Ribeiro, A.T.P. Melo, M. Vivan, A.M. Oliveira-Brett, In situ electrochemical and AFM study of thalidomide–DNA interaction, *Bioelectrochemistry* 76 (2009) 201–207.